

Dual Function of Protein Kinase C (PKC) in 12-O-Tetradecanoylphorbol-13-acetate (TPA)-induced Manganese Superoxide Dismutase (MnSOD) Expression

ACTIVATION OF CREB AND FOXO3a BY PKC- α PHOSPHORYLATION AND BY PKC-MEDIATED INACTIVATION OF Akt, RESPECTIVELY^{*[5]}

Received for publication, May 25, 2011, and in revised form, June 21, 2011. Published, JBC Papers in Press, June 24, 2011, DOI 10.1074/jbc.M111.264945

Youn Wook Chung^{#1}, Ha Kun Kim^{#2}, Ick Young Kim⁵, Moon B. Yim^{#3}, and P. Boon Chock^{#3}

From the [#]Laboratory of Biochemistry, NHLBI, National Institutes of Health, Bethesda, Maryland 20892 and the ⁵Laboratory of Cellular and Molecular Biochemistry, School of Life Science and Biotechnology, Korea University, Seoul 136-701, Korea

12-O-tetradecanoylphorbol-13-acetate (TPA) has been shown to induce transcriptional activation of human manganese superoxide dismutase (MnSOD) mRNA in human lung carcinoma cells, A549, mediated by a protein kinase C (PKC)-dependent activation of cAMP-responsive element-binding protein (CREB)-1/ATF-1-like factors. In this study, we showed that MnSOD protein expression was elevated in response to TPA or TNF- α , but not to hydrogen peroxide treatment. TPA-induced generation of reactive oxygen species (ROS) was blocked by pretreatment of the PKC inhibitor BIM and NADPH oxidase inhibitor DPI. Small interfering RNA (siRNA) experiments indicated that knocking down the NADPH oxidase components *e.g.* Rac1, p22^{phox}, p67^{phox}, and NOXO1 in A549 cells impaired TPA-induced MnSOD expression. To identify the PKC isozyme involved, we used a *sod2* gene response reporter plasmid, pSODLUC-3340-12E-C, capable of sensing the effect of TNF- α and TPA, to monitor the effects of PKC isozyme-specific inhibitors and siRNA-induced knockdown of specific PKC isozyme. Our data indicate that TPA-induced MnSOD expression was independent of p53 and most likely mediated by PKC- α , and - ϵ -dependent signaling pathways. Furthermore, siRNA-induced knock-down of CREB and Forkhead box class O (FOXO) 3a led to a reduction in TPA-induced MnSOD gene expression. Together, our results revealed that TPA up-regulates, in part, two PKC-dependent transcriptional pathways to induce MnSOD expression. One pathway involves PKC- α catalyzed phosphorylation of CREB and the other involves a PKC-mediated the PP2A catalyzed dephosphorylation of Akt at Ser⁴⁷³ which in turn leads to FOXO3a Ser²⁵³ dephosphorylation and its activation.

Manganese superoxide dismutase (MnSOD)⁴ is a nuclear-encoded antioxidant enzyme that is imported into the mitochondrial matrix (1), to catalyze the dismutation of superoxide radical anions (O₂⁻) into hydrogen peroxide (H₂O₂) and oxygen (2). MnSOD is considered as the primary defensive enzyme against oxidative stress within mitochondria (3). Targeted disruption of murine *sod2* causes dilated cardiomyopathy and neonatal lethality (4). In addition, a low level of MnSOD has been implicated in causing various human tumors (5), whereas its overexpression suppresses tumorigenicity (6, 7).

A number of studies have demonstrated the induction of MnSOD in various cell lines and tissues following oxidative stress induced by treatments with TNF- α (8–12), interleukin-1 (8, 10–12), lipopolysaccharide (10, 12), interferon- γ (11), 12-O-tetradecanoylphorbol-13-acetate (TPA) (12, 13), or irradiation (14, 15). The induction of MnSOD is transactivated via two parts of the *sod2* gene in various species following oxidative stress. One part is the 5'-flanking promoter region regulated by Sp-1 (16–18), and with early growth response factor (Egr-1) after treatment with TPA (19), or by AP-2 (16, 17, 20–22). The other part is the enhancer within the second intron regulated by the CCAAT/enhancer-binding protein (C/EBP) and NF- κ B in response to TNF- α and interleukin-1 (IL-1) (23, 24) or TPA (25, 26). We have previously identified the manganese superoxide dismutase TPA-responsive element (MSTRE), in the 5'-flanking region, located between -1292 and -1202, which contains a cAMP-responsive element (CRE)-like sequence, and demonstrated that CREB/ATF-1 bound to MSTRE and TPA treatment induced CREB phosphorylation (27).

It has been proposed that the tumor-promoting phorbol ester, TPA, (28, 29) induces MnSOD expression in a protein kinase C (PKC)-dependent manner (27, 30–32). Our previous study using A549 cells reveals that PKC may be involved in CREB phosphorylation (27), and another study has shown that transcription factor FOXO3a (also known as FKHL1) can elevate the expression of MnSOD in response to oxidative stress (33). In addition, FOXO transcription factors are known to trig-

* This work was supported, in whole or in part, by the Intramural Research Program of NHLBI, National Institutes of Health.

[5] The on-line version of this article (available at <http://www.jbc.org>) contains supplemental Figs. S1 and S2 and Tables S1–S3.

¹ Present address: Cardiovascular Pulmonary Branch, NHLBI, National Institutes of Health, Bethesda, MD 20892.

² Permanent address: Dept. of Life Science & Genetic Engineering, Pai Chai University, Daejeon, Korea, 302-735.

³ To whom correspondence should be addressed: Laboratory of Biochemistry, NHLBI, National Institutes of Health, Building 50, Room 2134, MSC-8012, Bethesda, MD 20892-8012. Tel.: 301-496-2073; Fax: 301-451-5459; E-mail: bchock@nih.gov.

⁴ The abbreviations used are: MnSOD, manganese superoxide dismutase; PKC, protein kinase C; CREB, cAMP-responsive element-binding protein; FOXO, Forkhead box class O; TPA, 12-O-tetradecanoylphorbol-13-acetate; ROS, reactive oxygen species; siRNA, small interfering RNA; PHLPP, PH domain leucine-rich repeat protein phosphatase.

Dual Function of PKC in TPA-induced MnSOD Expression

ger a variety of cellular processes by up-regulating a series of target genes, including *sod2*, in response to different cellular stresses (34). However, the mechanism by which PKC regulates MnSOD induction remains unclear.

In this study we investigated the roles of PKC in TPA-induced MnSOD in A549 cells. To this end we identified PKC- α as the PKC isozyme that catalyzes the phosphorylation of CREB. However, TPA treatment also causes a reduction in phosphorylated Akt (at Ser⁴⁷³) and FOXO3a (at Ser²⁵³), and the PKC inhibitor restored the phosphorylation level suppressed by TPA. In addition, we showed that knock-down of four components of NADPH oxidase diminished TPA-mediated MnSOD induction, suggesting that NADPH oxidase is involved in the early stage of MnSOD gene induction. This observation suggests to us that superoxide radical anions could be the upstream signal for TPA induction. Together, our data showed that PKC is involved in regulating the activation of transcription factors induced by TPA, via the phosphorylation of CREB on one hand and dephosphorylation of FOXO3a on the other hand.

EXPERIMENTAL PROCEDURES

Materials—DMSO, TPA, TNF- α , diphenyleneiodonium chloride (DPI), *N*-acetylcysteine (NAC), and 2',7'-dichlorofluorescein diacetate (DCFH-DA) were purchased from Sigma. From Calbiochem (La Jolla, CA), we purchased PKC inhibitors BIM, Gö6983, Gö6976, and Rottlerin; and protein phosphatase 1 and 2A (PP1 and PP2A) inhibitor okadaic acid. The PH domain leucine-rich repeat protein phosphatase (PHLPP) inhibitor, NCS 45586 (#13) was a generous gift from Dr. Alexandria C. Newton, at the University of California San Diego, La Jolla, CA (35).

Cell Line—The human lung adenocarcinoma cell line A549 (ATCC CCL-185) was purchased from American Type Culture Collection. Cells were cultured in RPMI 1640 (Invitrogen, Carlsbad, CA) supplemented with 10% fetal bovine serum (FBS) and antibiotics (Invitrogen) at 37 °C under 5% CO₂.

Subcellular Fractionations—Subcellular fractions were prepared from A549 cells according to Enoksson *et al.* (36) with minor modification (37). In brief, fresh or frozen cells were lysed in MSH buffer (210 mM mannitol, 70 mM sucrose, 5 mM Hepes, pH 7.5) in the presence of 1 mM EDTA, incubated for 30 min on ice and homogenized with a tight-fitting glass-Teflon motorized homogenizer (500 rpm, 30 strokes). Homogenates were centrifuged at 600 \times *g* for 8 min at 4 °C. The pellet was solubilized in lysis buffer (10 mM HEPES, pH 7.9, 10 mM KCl, 0.1 mM EDTA, 0.1 mM EGTA, 1 mM DTT, 0.5 mM PMSF, 2 μ g/ml leupeptin, and 2 μ g/ml aprotinin). After 30 min incubation on ice, 0.3% Nonidet P-40 was added, vortexed for 1 min, and centrifuged at 12,000 \times *g* for 1 min. The pellet was lysed with nuclear extraction buffer (25 mM HEPES, pH 7.9, 0.5 mM EDTA, 0.5 mM EGTA, 0.4 M NaCl, 1 mM DTT, 1 mM PMSF, 2 μ g/ml leupeptin, 2 μ g/ml aprotinin). After centrifugation at 12,000 \times *g* for 5 min at 4 °C, the nuclear fraction (supernatant) was collected. The supernatant from the first centrifugation was centrifuged at 5,500 \times *g* for 15 min to obtain the mitochondrial fraction. Membrane and cytosolic fractions were prepared as described previously (30).

Western Blotting and Immunoprecipitation—Samples were electrophoresed in 10–20% Tris-Glycine gels (Invitrogen) and transferred onto polyvinylidene difluoride (PVDF) membranes (Invitrogen). After incubating with Li-Cor Blocking Buffer (Li-Cor Biosciences, Lincoln, NE) for 30 min, blots were incubated with specific primary antibodies against PKC- α (polyclonal, C-20), PKC- β I (polyclonal, C-16), PKC- β II (polyclonal, C-18), PKC- δ (polyclonal, C-20), PKC- ϵ (polyclonal, C-15), PKC- μ (polyclonal, C-20), p53 (monoclonal, DO-1), or α -tubulin (monoclonal, TU-02) from Santa Cruz Biotechnology, Inc. (Santa Cruz, CA), or CREB (rabbit monoclonal, 48H2), phospho-CREB at Ser¹³³ (rabbit monoclonal, 87G3), FOXO3a, phospho-FOXO3a (Ser²⁵³), Akt (polyclonal), and phospho-Akt (Ser⁴⁷³, polyclonal) from Cell Signaling Technology (Danvers, MA), Rac1 (monoclonal, 05–389), and p67^{phox} (polyclonal, 07–502) from Upstate (Lake Placid, NY), NOXO1 (goat polyclonal, IMG-3062) from IMGEX (San Diego, CA), MnSOD (polyclonal, RDI-RTSODmAbR) from Fitzgerald (Concord, MA), mtHSP70 (monoclonal, MA3–028) from Affinity Bioreagents (Golden, Co), β -actin (monoclonal (AC-74)) from Sigma or Lamin B (NA12) from Calbiochem in Li-Cor Blocking Buffer containing 0.1% Tween 20 for overnight at 4 °C. Blots were then incubated with either goat anti-rabbit IRDye800CW secondary antibodies (611-731-127, Rockland Immunochemicals, Gilbertsville, PA) or goat anti-mouse Alexa Fluor 680 secondary antibodies (A21058, Molecular Probes, Eugene, OR) and visualized using Odyssey Infrared Imaging System (Li-Cor Biosciences).

For immunoprecipitation, cells were lysed in lysis buffer (Cell Signaling Technology) containing Complete Mini, protease inhibitor mixture tablets (Roche Diagnostics, Indianapolis, IN) and phosphatase inhibitor cocktails (Set II and VI, Calbiochem) and were incubated with either normal rabbit IgG (sc-2027, Santa Cruz Biotechnology), or rabbit monoclonal phospho-Akt at Ser⁴⁷³ (193H12) antibody (Cell Signaling Technology) for 1 h and followed by an additional 30 min of incubation with protein A-agarose (Millipore, Lake Placid, NY). Immunoprecipitation and 2% of total cell lysates separated by SDS-PAGE and transferred onto PVDF were then incubated with phospho-Akt (Ser⁴⁷³) (193H12) antibody or PP2A C subunit antibody (2038, Cell Signaling Technology).

Assessment of Intracellular ROS—Production of ROS was assessed by oxidation-sensitive fluorescent probe DCFH-DA as described previously (38). Hydrogen peroxide (1 mM) was used as a positive control. After washing twice with PBS to remove the extracellular dye, cells were analyzed with a flow cytometry (FACSCalibur, BD Biosciences, San Jose, CA). DCFH-DA fluorescence was excited at 488 nm, and the emission was monitored at 530 nm.

Dual Priming Oligonucleotide (DPO) PCR System—mRNAs from A549 cells were analyzed using dual priming oligonucleotide (DPO) PCR system (39). DPO primers for NADPH oxidase component ([supplemental Table S2](#)) and for PKC family ([supplemental Table S3](#)), and housekeeping gene primers (SM1001) were purchased from Seegene Institute of Life Science (Seoul, Korea). They included dual oxidase (DUOX) 1 and 2; p47^{phox} and its homologue Nox organizer 1 (NOXO1), p67^{phox} and its homologue and Nox activator 1 (NOXA1); p40^{phox}, Rac1, Rac2,

and p22^{phox}; classical PKC (PKC- α , - β I, - β II, and - γ), novel PKC (PKC- δ , - θ , - ϵ , and - η), atypical PKC (PKC- ζ and - λ), and PKD (PKC- μ).

Small-interfering RNA (siRNA)—Sixty hours after transfection with siRNAs (250 nM) using Amaxa Nucleofector System (Amaxa Biosystems, Gaithersburg, MD), cells were treated with TPA for the indicated times. In this study, both siGENOME SMART pool and ON-TARGETplus SMART pool (Dharmacon/Thermo Fisher, Chicago, IL) were used; Rac1 (M-003560-02), p22^{phox} (L-011020-00), p67^{phox} (L-004529-00), DUOX1 (L-008126-00), and NOXO1 (M-016237-00) for knockdown of NADPH oxidase components; PKC- α (L-003523-00), PKC- β I (L-003758-00), and PKC- δ (L-003524-00) for knockdown of PKC family; and CREB (L-003619-00), FOXO3a (L-003007-00) and p53 (M-003329-01, and M-003329-02 from Dharmacon; sc-29435 from Santa Cruz Biotechnology). A non-targeting pool was used as control RNA (ON-TARGETplus siCONTROL, Dharmacon).

Luciferase Assay—Small enhancer region in intron 2 of *sod2* gene (I2E), which is responsive to tumor necrosis factor- α (TNF- α) and interleukin-1 β (IL-1 β), was found in mouse (23) and in human (24). Combined with 3340 base pairs of 5'-flanking region of the human *sod2* gene promoter (27), three plasmids were constructed, in which I2E were located in N-terminal end (pSODLUC-3340-I2E-N) and C-terminal end (pSODLUC-3340-I2E-C) of the promoter, and between the promoter and the *luciferase* gene (*Luc*⁺) (pSODLUC-3340-I2E-ORF) (supplemental Fig. S1a). A549 cells were transfected with pSODLUC plasmids using Amaxa Nucleofector System. Twenty-four hours after transfection, cells were treated with TPA and incubated for another 24 h. The firefly and *Renilla* luciferase activities were measured using the Dual Luciferase assay system (Promega, Madison, WI).

Statistical Analysis—An unpaired two-tailed distribution Student's *t* test (Microsoft Excel) and a one-way ANOVA were used to analyze data, and results were expressed as means \pm S.E. A value of *p* < 0.05 was considered significant.

RESULTS

Induction of MnSOD in Mitochondria by TPA-mediated Production of Superoxide Radical Anion—Previously we showed that the induction of MnSOD mRNA by TPA treatment was mediated by the manganese superoxide dismutase TPA-responsive element (MSTRE) in the 5'-flanking region of the human MnSOD gene promoter (27). Fig. 1a shows that MnSOD protein in mitochondria was significantly elevated by treatment of A549 cells with either TPA or TNF- α , but not with the externally added 1 mM hydrogen peroxide. It should be pointed out that when A549 cells were incubated in the presence of 5 mM H₂O₂ for 24 h at 37 °C, the cells were found dead and detached. However, when the concentration of H₂O₂ was reduced to 0, 0.5, and 1 mM under similar experimental conditions the cells exhibited similar confluency. The effect of TPA is consistent with the observed increase in MnSOD mRNA level, while the effect of TNF- α is in agreement with that reported by Wong *et al.* (9) using a human embryonic kidney (HEK) 293 cell line. Together these data suggest that the reactive oxygen spe-

cies (ROS) produced by TPA or TNF- α treatments to induce MnSOD in mitochondria, is not H₂O₂.

The results in Fig. 1c show the intracellular concentration of ROS was elevated by 1.9-fold after A549 cells were treated with 32.4 nM (20 ng/ml) of TPA for 1 h. However this observed increase of intracellular ROS induced by TPA, monitored by DCF fluorescence, was suppressed either by PKC inhibitor BIM (1 μ M) or by NADPH oxidase inhibitor DPI (100 nM) (Fig. 1, b and c). It should be pointed out that DPI by itself causes a significant increase in ROS, a phenomenon due to DPI-elicited inhibition of cell redox metabolism and augmented oxidative stress (40). These results suggest that ROS produced in response to TPA is a superoxide radical anion (O₂⁻) generated by NADPH oxidase or flavoproteins in a PKC-dependent manner.

It is generally believed that TPA-induced ROS is mediated by PKC activation which in turn activates NADPH oxidase. To identify which components of NADPH oxidase are crucial in TPA-mediated MnSOD induction in A549 cells, a dual priming oligonucleotide (DPO) PCR system was used. As shown in Fig. 1d, we observed the mRNAs for p67^{phox}, NOXO1 (p47^{phox} homologue) NOXA1 (p67^{phox} homologue), DUOX1, Rac1, and p22^{phox} in A549 cells. However, mRNA for p40^{phox}, p47^{phox} (NCF1), Rac2, or DUOX2 was not detected. To show the effect of knocking down the observed components of NADPH oxidase, such as Rac1, p22^{phox}, p67^{phox}, and NOXO1, on TPA-induced MnSOD protein expression in A549 cells siRNA methods were used. Fig. 1e shows the efficiency of siRNA in reducing the protein level of Rac1, NOXO1 and p67^{phox}. The results in Fig. 1f show that knocking down Rac1, p22^{phox}, p67^{phox}, or NOXO1, each contributes to a reduction of 30% in the amplitude of TPA-induced MnSOD expression, relative to that obtained with control siRNA-transfected cells. These results suggest that not only cytosolic regulatory factors, such as p67^{phox}, NOXO1 (p47^{phox}), and Rac1, but membrane-bound p22^{phox} is also required to induce MnSOD expression.

PKC-dependent TPA-mediated MnSOD Induction—To investigate which PKC isozyme is responsible for the TPA induced MnSOD in A549 cells, the PKC isozymes in these cells were identified using the DPO PCR method (Fig. 2a). These results reveal that PKC- α , - β I, - β II, - γ , - δ , - θ , - ϵ , - η , - ζ , - λ , and - μ , are expressed in A549 cells. Fig. 2b shows the effect of TPA and H₂O₂ on the activation and membrane translocation of PKC isozyme in A549 cells. Using six different PKC polyclonal antibodies, we detected that PKC- α , - β I, - δ , - ϵ , and - μ (PKD) but not PKC- β II were translocated to the membrane fractions in TPA-treated cells. Interestingly none of these PKC isoforms was affected by H₂O₂ treatment. The TPA-mediated translocations of PKC- α , - β I, - δ , and - ϵ to the membrane fraction were somewhat similar to those in the previous study (30), except in our hands the membrane translocation of PKC- α is much more robust and the membrane translocated PKC- μ appeared to be covalently modified since the band is more diffused and migrated at a slower rate.

To assess the effect of a PKC inhibitor on the TPA-induced transcription of *sod2*, a luciferase reporter plasmid was used. Because MnSOD was induced by TPA and TNF- α (Fig. 1a), and the pSODLUC-3340 plasmid did not respond to TNF- α treatment (27), new plasmids, which include the intron 2 enhancer

Dual Function of PKC in TPA-induced MnSOD Expression

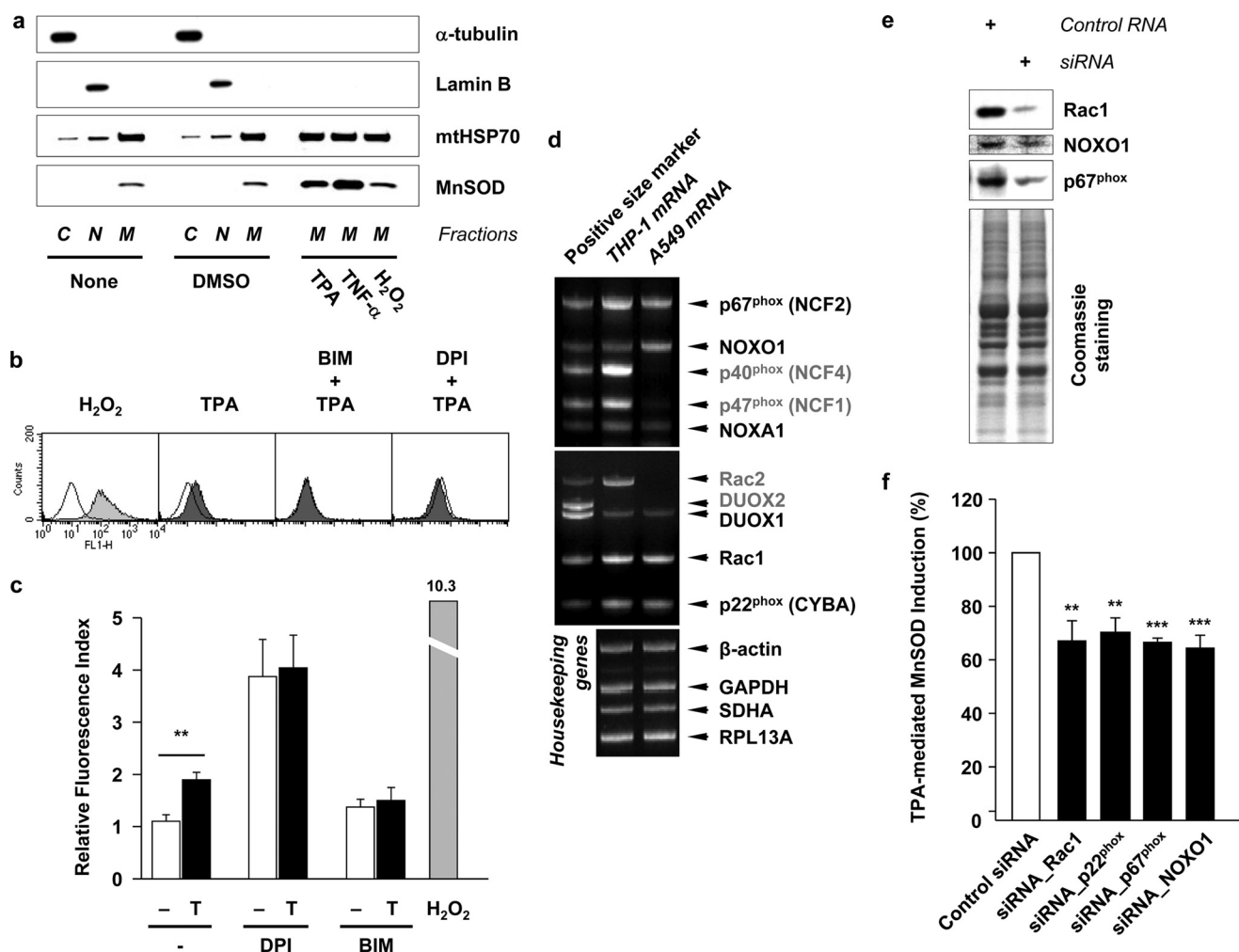


FIGURE 1. Superoxide radical anion generated by NADPH oxidase in response to TPA induces MnSOD in mitochondria. *a*, A549 cells were fractionated into cytosolic (C, α -tubulin as a marker), nuclear (N, LaminB as a marker), and mitochondrial (M, mtHSP70 as a marker) fractions after treatment of TPA (32.4 nM, 20 ng/ml), TNF- α (10 ng/ml) or hydrogen peroxide (H₂O₂) (1 mM) for 24 h at 37 °C. Each fraction sample was separated using 10–20% Tris-glycine gel and analyzed by immunoblotting. *b*, after incubation with either PKC inhibitor BIM (1 μ M) or NADPH oxidase inhibitor DPI (100 nM) for 1 h, cells were treated with TPA for 30 min. The cells were further incubated in the presence of 40 μ M 2',7'-dichlorofluorescein diacetate (DCFH-DA) for 30 min at 37 °C. Stained cells were washed with PBS and analyzed by flow cytometry (FACS). H₂O₂ (1 mM) was treated as a positive control. *c*, DCF fluorescence index was presented as a ratio to the cells not exposed to both inhibitors and TPA (T). Values are means \pm S.E. ($n \geq 4$, **, $p < 0.01$). *d*, components of NADPH oxidase in A549 cells are examined by dual priming oligonucleotide (DPO) PCR system (missing components in A549 cells are presented as *gray letters*). For the data in *e* and *f*, small interfering RNA (siRNA) for Rac1, p22^{phox}, p67^{phox}, and NOXO1 (250 nM each) were used to knockdown each component of NADPH oxidase, which exist in A549 cells. Sixty hours after transfection of siRNAs, cells were treated with TPA for additional 24 h at 37 °C. *e*, Western blots for Rac1, NOXO1 and p67^{phox} after knockdown by each siRNAs. Coomassie-stained gel shows that equal amounts of sample were loaded. *f*, inhibitory effect of siRNAs on the TPA-mediated MnSOD induction was presented as a percentage to the MnSOD induction in cells transfected with control siRNA and treated with TPA. Values are means \pm S.E. ($n \geq 3$, **, $p < 0.01$ and ***, $p < 0.001$ versus control siRNA by ANOVA; *n.s.*, not significant).

(I2E) fragment, known as a responsive element to TNF- α in murine (23) and human (24), were constructed. The three plasmids shown in [supplemental Fig. S1a](#) were constructed as described under "Experimental Procedures." The new plasmids allow one to monitor the possible synergic effect of I2E on TPA-mediated luciferase activity. [supplemental Fig. S1b](#) shows that A549 cells transfected with pSODLUC-3340 plasmid did not exhibit any increase in luciferase activity due to TNF- α treatment. However, cells transfected with pSODLUC-3340-I2E-C, -N, and -ORF plasmids induced *sod2* reporter gene expression by 2.4-, 3.6-, and 3.5-fold, respectively, due to TNF- α treatment, consistent with previous reports (23, 27). Moreover, the insertion of I2E also enhanced the TPA-mediated luciferase activity by 6.1-fold (pSODLUC-3340-I2E-C), 8.5-fold (pSODLUC-3340-I2E-N) and 5.3-fold (pSODLUC-3340-I2E-ORF)

([supplemental Fig. S1b](#)). Because I2E of pSODLUC-3340-I2E-C is located at a similar distance from the promoter as the original site of I2E and only pSODLUC-3340-I2E-C construct showed the inhibitory effect of Rottlerin (data not shown), it was selected for further promoter studies. To identify the effective PKCs, among those activated and translocated to membrane fraction by TPA, on MnSOD induction, four different PKC inhibitors, BIM (1 μ M), Rottlerin (5 μ M), Gö 6983 (1 μ M), and Gö 6976 (1 μ M), were used. Their K_i or IC₅₀ for a given PKC isozyme are summarized in [supplemental Table S1](#). Fig. 2c shows that treatment with 20 ng/ml of TPA causes a 7-fold increase in transcription activation of *sod2* and this induction was blocked by all four PKC inhibitors used and by DPI. Among the PKC inhibitors, general PKC inhibitors, BIM and Gö 6983 are the most potent relative to Gö 6976, which inhibits PKC- α

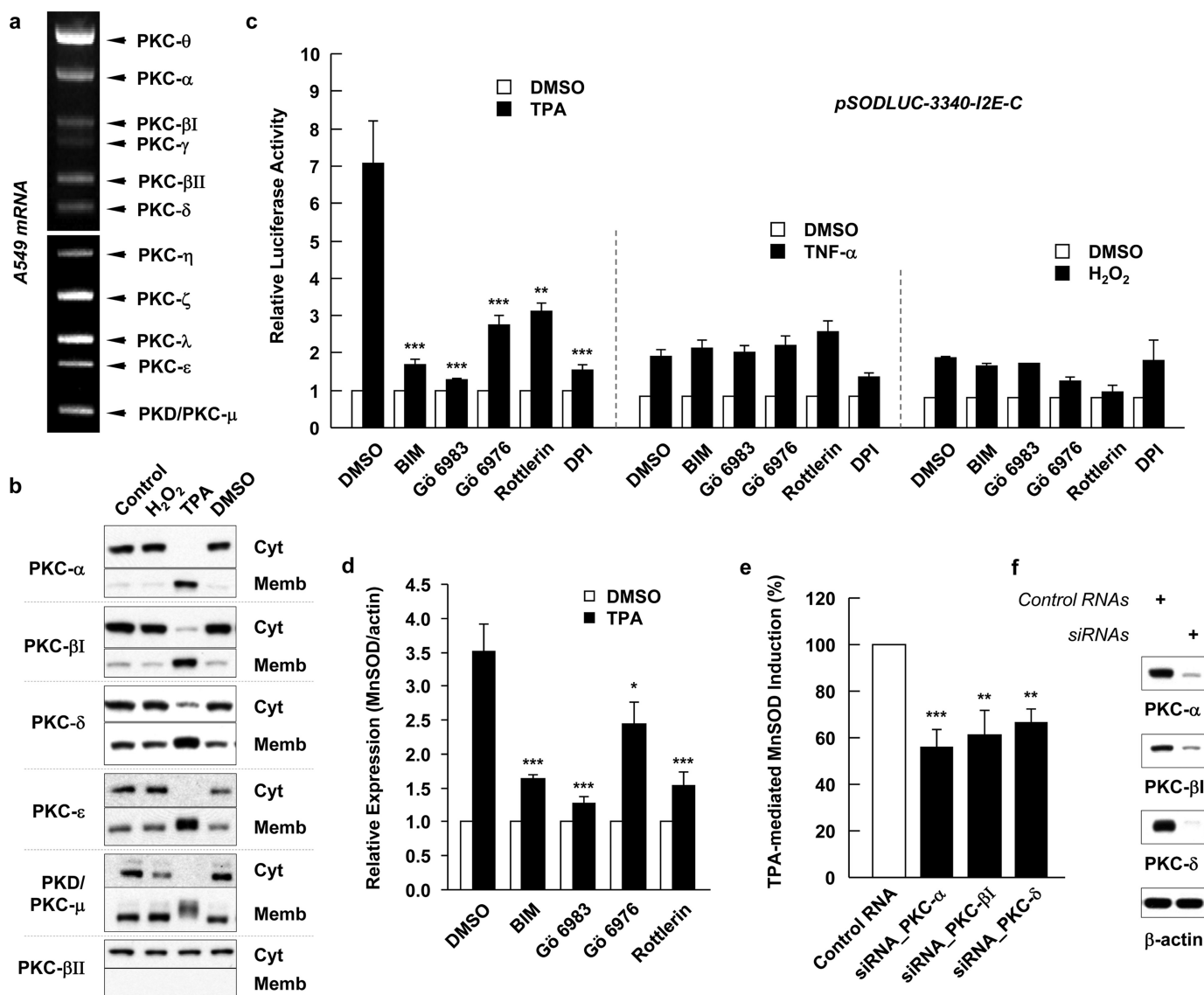


FIGURE 2. TPA-induced MnSOD expression was blocked by PKC inhibitors and siRNA knockdown on specific isozyme. *a*, in A549 cell, PKC isoforms were identified using DPO PCR system. *b*, translocations of PKCs to subcellular membrane were analyzed by immunoblotting after treatment with 32.4 nM TPA or 1 mM H₂O₂ for 30 min. Cyt, cytosolic fraction; Memb, membrane fraction. *c*, A549 cells were preincubated with BIM (1 μ M, inhibits PKC- α , - β I, - β II, - γ , - δ , and - ϵ), Gö 6983 (1 μ M, inhibits PKC- α , - β I, - β II, - γ , - δ , and - ζ), Gö 6976 (1 μ M, inhibits PKC- α , - β I, and - μ), or Rottlerin (5 μ M, inhibits PKC- δ and - θ) and treated with 32.4 nM TPA, 10 ng/ml of TNF- α or 1 mM H₂O₂ for 24 h. The effect of PKC inhibitors on the TPA-, TNF- α -, or H₂O₂-induced reporter gene activity was presented as relative luciferase activities to its activities in cells transfected with pSODLUC-3340-I2E-C and treated with the same volume of DMSO (vehicle) used in other samples. Values shown are means \pm S.E. ($n \geq 4$, ** $p < 0.01$ and *** $p < 0.001$ versus TPA-only treated group by ANOVA). *d*, after treatment as described previously, whole cell lysates were subjected to SDS-PAGE and blotted with anti-MnSOD antibody. The effect of PKC inhibitors on the TPA-mediated MnSOD induction was presented as a ratio to the MnSOD induction in cells pretreated with DMSO and then treated with TPA. Values are means \pm S.E. ($n \geq 3$, * $p < 0.05$ and *** $p < 0.001$ versus TPA-only treated group by ANOVA). *e*, inhibitory effect of siRNAs for PKC- α , - β I, and - δ (250 nM each) on the TPA-mediated MnSOD induction was presented as a percentage to the MnSOD induction in cells transfected with control siRNA and treated with TPA. ($n \geq 6$, ** $p < 0.01$ and *** $p < 0.001$ versus control siRNA by ANOVA). *f*, reduction of PKC- α , - β I, and - δ protein expression by siRNA.

and - β I, and to Rottlerin. However, *sod2* gene expression in response to TNF- α or H₂O₂ treatment was not significantly inhibited by any PKC inhibitors or DPI.

Fig. 2*d* shows that TPA-induced MnSOD protein generation was also inhibited by the PKC inhibitors. BIM and Gö 6983 yielded a 53.5 and 63.8% inhibition, respectively; while Gö 6976 and Rottlerin yielded a 30.1 and 56.3% inhibition, respectively. The effect of an individual PKC isozyme on the TPA-induced MnSOD generation was also investigated using the siRNA knockdown method. In this case, the siRNAs for PKC- α , PKC- β I and PKC- δ were transfected to reduce their expression.

The effectiveness of the knockdown is shown in Fig. 2*f*. The inhibitory effects of knocking down PKC- α , - β I, and - δ are shown in Fig. 2*e*. The results indicated that knocking down PKC- α , - β I, and - δ individually leads to 44.2, 38.9, and 33.5% inhibition respectively of TPA-induced MnSOD formation.

TPA-induced PKC- α -catalyzed CREB Phosphorylation—Previously we reported that transcription activation of MnSOD in A549 cells induced by TPA is mediated via the binding of MSTRE to a CREB-1/ATF-1-like transcription factor, which is activated by PKC-catalyzed phosphorylation of CREB at Ser¹³³ (27). The participation of CREB in the TPA-mediated MnSOD

Dual Function of PKC in TPA-induced MnSOD Expression

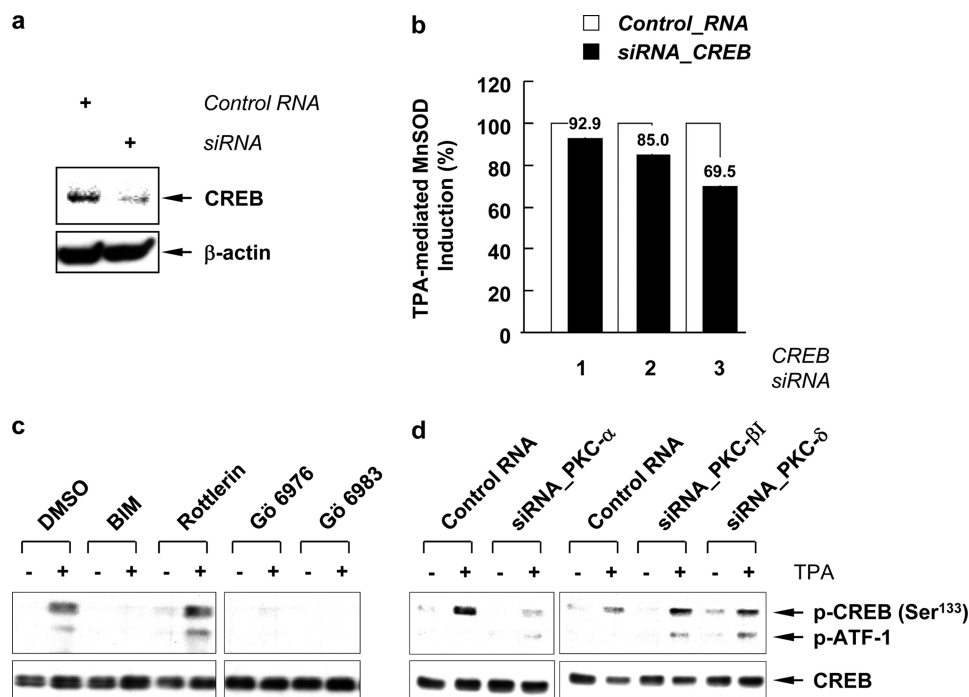


FIGURE 3. Phosphorylation of CREB catalyzed by PKC in TPA mediated MnSOD induction. *a*, Western blots for CREB after knockdown by siRNA. *b*, inhibitory effect of CREB siRNA on the TPA-mediated MnSOD induction was presented as a percentage to the MnSOD induction in cells transfected with control siRNA using the Amaxa Nucleofector System and treated with TPA. *Lane 1*, transfected with 100 nM siRNA for 48 h; *lanes 2 and 3*, transfected with 250 nM siRNA for 48 h in *lane 2* and 60 h in *lane 3*. *c*, cells were pretreated with BIM (1 μ M), Gö 6983 (1 μ M), Gö 6976 (1 μ M), or Rottlerin (5 μ M) for 1 h and treated with TPA for 30 min. *d*, siRNA for PKC- α , - β 1, and - δ (100 nM each) were used to knockdown each gene product. Two days after transfection of siRNAs, cells were treated with TPA for 30 min. Total cell lysates were subjected to SDS-PAGE and blotted with phospho-CREB (Ser¹³³) and CREB antibodies.

induction was further determined using siRNA technique. When siRNA for CREB was transfected into A549 cells, it successfully reduced the CREB protein (Fig. 3*a*). The reduction of the CREB protein led to a 30.5% suppression of the TPA-mediated MnSOD induction at 60 h (Fig. 3*b*). To link the upstream PKCs with the downstream transcription factors, we examined the effect of PKC inhibitors or siRNA on the phosphorylation of CREB. When cells were pretreated with BIM, Gö 6983, or Gö 6976, the TPA-stimulated phosphorylations of CREB were completely eliminated by inhibitors of classical PKCs, but not by Rottlerin, an inhibitor of PKC- δ and - θ (Fig. 3*c*). In addition, knockdown of PKC- α by siRNA also abolished CREB phosphorylation (Fig. 3*d*), while the reduction of PKC- β 1 and PKC- δ had no effect on the TPA-mediated phosphorylation of CREB. These data suggest that TPA-stimulated phosphorylation of CREB is mediated by PKC- α , and other PKCs induce expression of MnSOD by a path that does not involve CREB.

PKC-dependent Dephosphorylation of Akt and FOXO3a Induced by TPA Treatment—It has been shown that MnSOD protein expression is regulated by a PI3K-Akt-Forkhead signaling pathway (33). Compared with other transcription factors, the molecular mechanism by which Forkhead transcription factors regulates MnSOD gene expression after TPA treatment is not well characterized. In order to examine whether the Forkhead transcription factor FOXO3a (FKHRL1) is involved in the TPA-mediated MnSOD induction, siRNA for FOXO3a was transfected to block its expression. Fig. 4*a* shows that siRNA for FOXO3a successfully abolished its target protein. As a result of the FOXO3a knockdown, TPA-mediated MnSOD induction was inhibited by up to 40.2% (Fig. 4*b*). Fig. 4*c* shows that in the

nuclear fraction, TPA treatment led to the dephosphorylation of Ser²⁵³ in FOXO3a within 30 min.

Because Akt is a known upstream kinase for FOXO3a (41), we next investigated the phosphorylation of Akt after TPA treatment. Fig. 4*d* shows that Akt phosphorylation at Ser⁴⁷³ decreased due to serum starvation and elevated rapidly due to insulin treatment. In contrast, Akt phosphorylation decreased dramatically within 15 min induced by TPA treatment and sustained for up to 24 h (data not shown). These observations are in accord with the reports showing that TPA attenuated Akt phosphorylation in A549 cells (42) and PKC- δ and PKC- ϵ negatively regulated the phosphorylation of Akt in mouse keratinocytes (43). To investigate the effect of PKC on the dephosphorylation of Akt and FOXO3a, cells were preincubated with BIM and then treated with TPA. As shown in Fig. 4, *e* and *f*, the TPA-stimulated dephosphorylation of Akt at Ser⁴⁷³ and of FOXO3a at Ser²⁵³ were restored in a BIM concentration-dependent manner. These results suggest that the dephosphorylation of Akt and FOXO3a is mediated by PKC.

The phosphorylated Akt at the hydrophobic motif Ser⁴⁷³ is known to be dephosphorylated by okadaic acid-sensitive phosphatases such as PP2A (44–47) and by PHLPP (48). To differentiate which of these family of phosphatases is involved in regulating the activity of Akt mediated by TPA treatment, A549 cells were treated with either PP1 and PP2A inhibitor okadaic acid (46) or PHLPP inhibitor NCS 45586 (35). Fig. 5*a* shows that the dephosphorylation of Akt was inhibited by preincubation with okadaic acid in a dose-dependent manner. However NCS 45586 failed to inhibit Akt dephosphorylation (Fig. 5*b*). To investigate the mechanism by which PKC mediated the

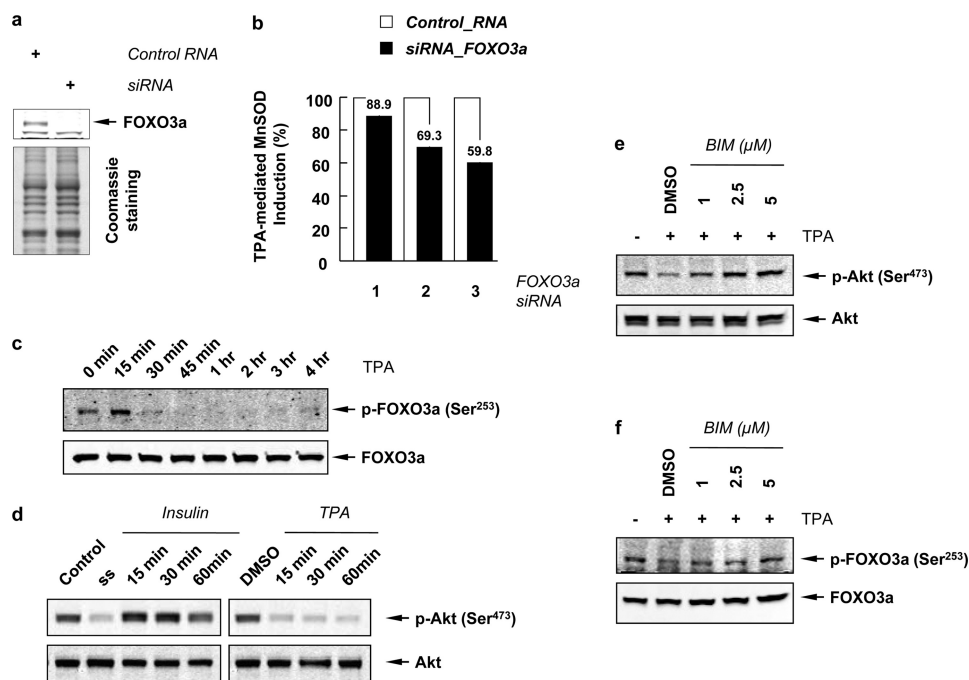


FIGURE 4. TPA induces the dephosphorylation of Akt and FOXO3a in a PKC-dependent manner. *a*, Western blots for FOXO3a after knockdown by siRNA. Coomassie-stained gel shows that equal amounts of sample were loaded. *b*, inhibitory effect of FOXO3a siRNA on the TPA-mediated MnSOD induction is presented as percent of MnSOD generated relative to that observed with control siRNA. Lane 1, transfected with 100 nM siRNA for 48 h; lanes 2 and 3, transfected with 250 nM siRNA for 48 h in lane 2 and 60 h in lane 3. *c*, nuclear fractions of A549 cells treated with TPA for the indicated time (up to 4 h), were separated in 8% Tris-glycine gel, and blotted with phospho-FOXO3a (Ser²⁵³) and FOXO3a antibodies. *d*, phosphorylation of Akt was examined by Western blotting using phospho-antibody against Ser⁴⁷³ residue of Akt after treated serum-starved (ss) cells with insulin (200 nM) (left panel) or TPA (right panel). *e* and *f*, A549 cells were preincubated with BIM (1, 2.5, and 5 μ M) for 1 h and treated with TPA for an additional 1 h. Total cell lysates were blotted with phospho-Akt (Ser⁴⁷³) and Akt antibodies (*e*), and nuclear fractions were blotted with phospho-FOXO3a (Ser²⁵³) and FOXO3a antibodies (*f*). Note that these blots represent one of three independent experiments.

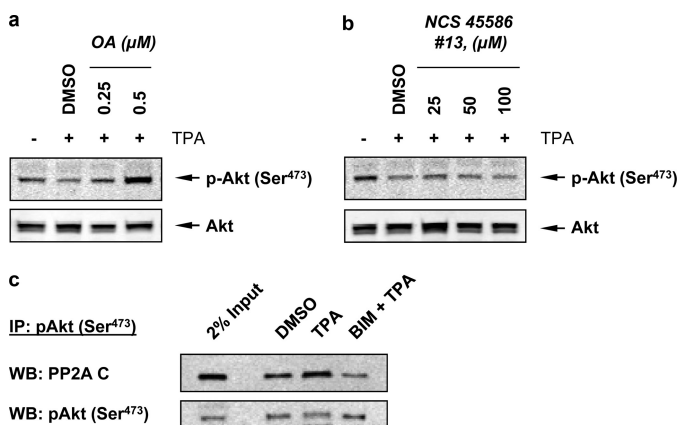


FIGURE 5. TPA induces PKC-mediated Akt dephosphorylation catalyzed by PP2A and not by PHLPP. Cells were pretreated with either PP2A inhibitor okadaic acid (OA) (*a*), or PHLPP inhibitor NCS 45586 (#13) (*b*) for 1 h, and then treated with TPA for another 1 h. Total cell lysates were blotted with phospho-Akt (Ser⁴⁷³) and Akt antibodies. *c*, cells treated with DMSO (vehicle), TPA only, or BIM plus TPA were lysed, and immunoprecipitation (IP) was performed using phospho-Akt (Ser⁴⁷³) antibodies. The immunoprecipitants and total cell lysates were analyzed by Western blotting (WB) for phospho-Akt (Ser⁴⁷³) and PP2A C subunit. Two percentages of total cell lysates were saved before IP and were also immunoblotted as a control (2% Input). Note that these blots represent one of three independent experiments.

dephosphorylation of Akt catalyzed by PP2A, we observed that TPA induced immuno-coprecipitation of pAkt complex with the catalytic subunit of PP2A and BIM inhibited the complex formation (Fig. 5*c*). This observation is in accord with the finding of Li *et al.* using mouse keratinocytes (43). Together, these results suggest that PKC induces the complex formation

between pAkt and the catalytic subunit of PP2A to facilitate the dephosphorylate Akt, which in turn activates FOXO3a by reducing the population of the phosphorylated FOXO3a at Ser²⁵³.

TPA-induced MnSOD Expression in A549 Cells Is Independent of p53—p53 has been shown to suppress MnSOD mRNA and protein levels by forming a complex with the Sp1 site at the 5'-flanking promoter region of the *sod2* gene and led to the reduction of transcription activity under both the constitutive and TPA-stimulated conditions in human hepatoma cell line HepG2 (18). With A549 cells, TPA induced a time-dependent reduction of p53 protein, while the MnSOD protein was elevated (Fig. 6*a*). A histochemical analysis revealed that the observed reduction of p53 was due to its translocation from the nucleus to the cytosol to be degraded (Fig. 6*b*). This TPA-mediated translocation and degradation of p53 was blocked by pretreatment of the cells with a potent and membrane permeable proteasome inhibitor, MG132, and a nuclear export inhibitor, leptomycin B (LMB) (data not shown). This apparent correlation, which could lead one to conclude that p53 also suppresses MnSOD expression in A549 cells, was uncoupled with experiments using siRNA to reduce the p53 protein expression. The results shown in Fig. 6*c* reveal p53 siRNA effectively lowering the p53 protein. However it exhibits little differential effect on the level of MnSOD protein expression in the absence or presence of p53. The quantitative effect of p53 siRNA knockdown is shown in Fig. 6*d*. Together these results indicate that while the variation of p53 and MnSOD induced by

Dual Function of PKC in TPA-induced MnSOD Expression

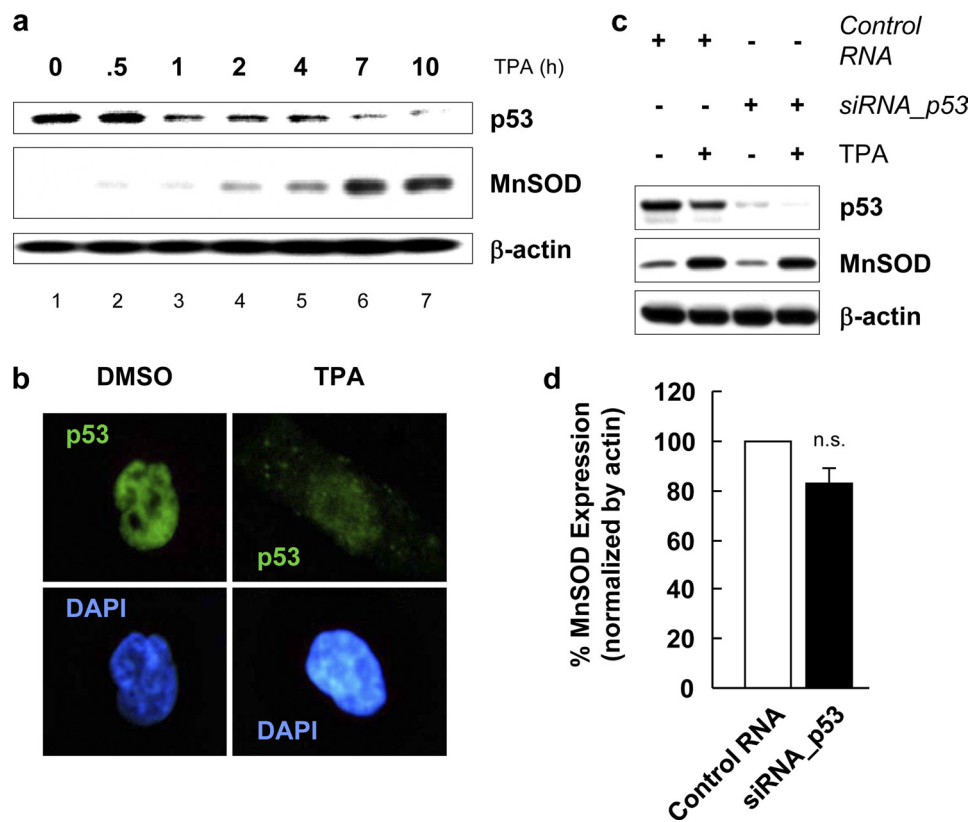


FIGURE 6. p53 is not a suppressor of MnSOD gene expression in human lung adenocarcinoma cell line A549. *a*, whole lysates of A549 cells treated with TPA for the indicated time period (up to 10 h), were separated in 10% Tris-glycine gel, and blotted with anti-p53 and anti-MnSOD antibodies. *b*, after TPA treatment, A549 cells on microscope slides in 6-well plates were fixed with 4% paraformaldehyde for 15 min at room temperature, permeabilized with 0.1% Triton X-100 for 5 min, and incubated with 2% BSA for 1 h to block nonspecific staining. The cells were then immunostained with anti-p53 antibody in 2% BSA for 1 h at room temperature and further incubated with fluorescence-conjugated secondary antibodies (Jackson ImmunoResearch, West Grove, PA) for 1 h at room temperature. To visualize nuclei, the cells were stained with 4',6'-diamidino-2-phenylindole (DAPI, Sigma) for 5 min. Finally, the cells were mounted onto slides using FluoroGuard antifade reagent (Bio-Rad). Immunofluorescence was examined using fluorescence microscope Axiovert (Carl Zeiss, Oberkochen, Germany). *c*, effect of p53 siRNA on the TPA-mediated MnSOD induction was monitored by Western blotting. *d*, quantitative effect of p53 siRNA on the TPA-induced MnSOD production is shown as percent MnSOD formed normalized by actin, with the value of 100% set for cells transfected with control siRNA followed with TPA treatment. Values shown are means \pm S.E. ($n = 3$, *n.s.*, not significant).

TPA suggests that p53 suppresses MnSOD expression in A549 cells, the siRNA data suggest otherwise, that p53 does not suppress MnSOD expression.

DISCUSSION

Phorbol esters, the pharmacological analogs of DAG, act as tumor promoters through activation of PKC. Among them TPA is the most widely used in models to study carcinogenesis (28). In this study, we investigated the mechanism by which TPA induces expression of MnSOD, a primary anti-oxidant enzyme, expression in A549 cells. p53, a tumor suppressor, has been reported to function as a pro-apoptotic factor under cellular response to stress conditions, and it has been shown that *p53* and *sod2* genes are reciprocally regulated in HepG2 and MCF-7 cells (18, 49). However, despite the fact that our data also revealed an apparent reciprocal effect on the expression of p53 and MnSOD induced by TPA treatment, the results obtained from the siRNA study are inconsistent with the notion that p53 suppresses MnSOD expression (Fig. 6, *c* and *d*). The reduction of p53 protein observed was caused by the TPA-mediated translocation of p53 from the nucleus to the cytosol for degradation.

We have previously shown that TPA induced MnSOD expression was blocked by inhibitors of flavoproteins and

NADPH oxidase suggesting that superoxide radical anion generation is likely an upstream signal (27). Here we show that A549 cell contains a number of components needed for constituting the reactive NADPH oxidase (Fig. 1*d*). In accord with the notion that the super oxide radical anion is an upstream signal, the results of siRNA knockdown of Rac1, p67^{phox}, and NOXO1 (p47^{phox}) significantly reduced the amplitude of MnSOD expression, while hydrogen peroxide failed to support the TPA-induced MnSOD generation.

It has been demonstrated that transcriptional activation of *sod2* mediated by TPA in A549 cells involves the binding of CREB-1/ATF-1-like transcription factor to a CRE-related sequence, MSTRE, in the promoter region of the gene (27). However TPA treatment did not lead to any change in the abundance or binding activity of CREB-1/ATF-1 complexes. This observation is in accord with the known behavior of CREB as a signal-dependent activator, whose trans-activation potential is specifically affected by phosphorylation instead of its nuclear targeting or its DNA binding activity (50). The transcription factor, CREB, is known to be regulated by a number of protein kinases, including PKA and PKC (51, 52). Because we found that the specific inhibitor for PKC, BIM, rather than the PKA inhibitor, H89, blocked the TPA-mediated induction of

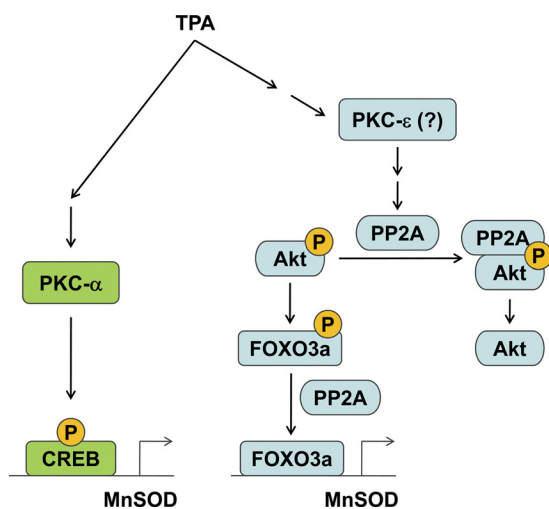


FIGURE 7. A simplified pathway to depict the TPA-induced MnSOD expression in A549 cells. Here TPA was shown to activate PKC- α , which in turn phosphorylates the CREB transcription factor, and PKC- ϵ , which induces the formation of PP2A-pAkt complex to facilitate the dephosphorylation of pAkt and subsequently lead to the accumulation of the dephosphorylated and active FOXO3a.

MnSOD mRNA (27), we used different PKC inhibitors and siRNA techniques to knockdown specific PKC isoforms in an attempt to identify the PKC isoform which catalyzes the phosphorylation of CREB in response to TPA treatment. The results show that knocking down PKC- α leads to a 44.2% reduction in TPA-induced MnSOD expression (Fig. 2e). Under these conditions, the phosphorylation of CREB at Ser¹³³ is nearly eliminated (Fig. 3, c and d). Together these results indicate that PKC- α is the PKC isoform that catalyzes the phosphorylation of CREB and lead to its transcriptional activation in response to TPA treatment (Fig. 7). In addition, the data in Fig. 2e show that knocking down PKC- δ and PKC- β also leads to a reduction of MnSOD expression. However the PKC- δ inhibitor Rottlerin and the siRNA knockdown of PKC- β and of PKC- δ exhibit little effect on CREB Ser¹³³ phosphorylation. Nevertheless, PKC- δ has been shown to up-regulate the NF- κ B-mediated MnSOD induction pathway (26, 30, 31).

The mammalian FOXO family of Forkhead transcription factors contains four family members, namely: the FOXO1/FKHR, FOXO3/FKHRL1, FOXO4/AFX, and FOXO6. They play an important role in longevity and growth/tumor suppression by up-regulating target genes involved in stress response (e.g. MnSOD), metabolism, cell cycle arrest (p21^{Waf1/Cip1} and p27^{Kip1}), DNA repair (GADD45 and DDB1), apoptosis, and autophagy (Bim and FasL) (34, 53). In our study, we found that A549 cells were arrested at G1 phase after 24 h of TPA treatment (supplemental Fig S2a), with an increase in the levels of p27^{Kip1}, GADD45, FasL, as well as MnSOD. Among them, MnSOD was the only target gene whose induction by TPA was blocked by BIM (supplemental Fig S2b). These observations indicate that TPA induces FOXO transcription factor activation in A549 cells to trigger up-regulation of target genes. They include *p27*, *fasl*, *gadd45*, and *sod2*, and the induction of *sod2* is inhibited by PKC inhibitor, BIM. The increase of p27^{Kip1} may, in part, be responsible for the observed cell cycle arrest at G1 phase (54). Furthermore, siRNA knockdown of CREB and FOXO3a

led to a 30.5, and a 40.2% inhibition, respectively, (Figs. 3b and 4b) in TPA-mediated MnSOD induction. Together, these results indicate that PKC is also involved in up-regulating FOXO3a transcription activity.

The activity of FOXO3a is regulated by reversible covalent modification, including reversible phosphorylation at three conserved residues, Thr³², Ser²⁵³, and Ser³¹⁵. The phosphorylation is catalyzed by Akt, GSK, and AMPK, while the dephosphorylation is catalyzed by PP2A (34, 47). Because Ser²⁵³ overlaps with the nuclear localization signaling (NLS) sequence, phosphorylation on this residue will likely interfere with nuclear import by disrupting the positively charged NLS, and impair its ability to react with its target genes. Akt, a known kinase that phosphorylates FOXO3a at Ser²⁵³, is activated by the phosphorylation of its Ser⁴⁷³. The dephosphorylation of Ser⁴⁷³ is catalyzed by PP2A (44, 45, 47) and by PHLPP (48). Experiments using overexpression of Akt and PHLPP in 293T cells or overexpression of PHLPP in H157 or MDA-MB-231 cells revealed that PHLPP specifically dephosphorylated pSer⁴⁷³ relative to pThr³⁰⁸ in Akt (48). However, the specificity for the dephosphorylation of pSer⁴⁷³ and pThr³⁰⁸ by PP2A appears to be regulated by the nature of its B regulatory subunit (45, 55). PP2A-B55 and PP2A-B56 holoenzymes have been shown to preferentially dephosphorylates pThr³⁰⁸ and pSer⁴⁷³, respectively. Under our experimental conditions, pAkt (Ser⁴⁷³) was dephosphorylated by okadaic acid-sensitive PP2A and not by PHLPP (Fig. 5, a and b). Therefore for PKC to activate FOXO3a, it must somehow activate PP2A activity. To this end, we found that TPA induces a complex formation between the phosphorylated Akt and the catalytic subunit of PP2A, and the stability of this complex is mediated by the activity of PKC (Fig. 5c). This observation is in accord with reports showing that activation of PKC- δ and PKC- ϵ provides a negative regulation for Akt phosphorylation and its kinase activity in mouse keratinocytes and TPA stimulated the association PP2A with Akt (43).

Investigating which of the PKC isoforms, PKC- δ or PKC- ϵ or both, is responsible for inducing the PP2A-mediated dephosphorylation of pAkt (Ser⁴⁷³) and pFOXO3a (Ser²⁵³), we found that BIM, a PKC inhibitor for PKC- α , - β I, - β II, - γ , and - ϵ , inhibited the TPA-induced dephosphorylation of pAkt (Ser⁴⁷³) and pFOXO3a (Ser²⁵³) in a concentration dependent manner (Fig. 4, e and f). However, when A549 cells were pre-treated with either 1 μ M Gö 6976, which inhibits PKC- α and - β I, or with 5 μ M Rottlerin, an inhibitor for PKC- δ and - θ , no inhibition of TPA-induced dephosphorylation of pAkt (Ser⁴⁷³) and pFOXO3a (Ser²⁵³) was detected (data not shown). Because TPA does not activate PKC- β II (Fig. 2b), an isoform inhibited by BIM, that leaves PKC- ϵ and PKC- γ as the only PKC isoforms inhibited by BIM but not by Gö 6976 and Rottlerin. Between these two PKC isoforms, PKC- ϵ has been shown, together with PKC- δ , as the PKC isoforms negatively regulated the phosphorylation of Akt and its kinase activity in mouse keratinocytes (43). However, PKC- δ can be ruled out because Rottlerin failed to inhibit TPA-induced Akt dephosphorylation. Therefore PKC- ϵ is likely the PKC isoform responsible for mediating the dephosphorylation of Akt and FOXO3a (Fig. 7). This simplified model depicted in Fig. 7 shows that activation of PKC- ϵ would lead to complex formation between PP2A and pAkt to facilitate

Dual Function of PKC in TPA-induced MnSOD Expression

the dephosphorylation of pAkt and pFOXO3a and lead to transcriptional activation of FOXO3a.

In summary, the elevation of MnSOD expression was mediated by NADPH oxidase pathway in A549 cells in response to TPA or TNF- α treatment, while treatment with external hydrogen peroxide fails induce a similar effect. In addition, while the effects of TPA on MnSOD induction and on p53 suppression appear to suggest that p53 suppresses MnSOD expression, our results from siRNA knockdown of p53 indicate otherwise, namely that p53 does not suppress MnSOD expression. Furthermore, the TPA-induced MnSOD generation was abolished by a general PKC inhibitor, BIM. Using various PKC isozyme inhibitors and siRNA knockdown methods, we reveal that TPA-induced MnSOD expression is, in part, regulated by a PKC- α -catalyzed phosphorylation of CREB transcription factor, and by a PKC mediated dephosphorylation of Akt at Ser⁴⁷³ catalyzed by PP2A, which in turn lead to FOXO3a dephosphorylation at Ser²⁵³. Thus, PKC, activated by a TPA-mediated pathway, is involved in activating at least two transcription factors, one via the phosphorylation of CREB and the other via a PKC-mediated dephosphorylation of Akt and FOXO3a by PP2A.

Acknowledgment—We thank Dr. Alexandria C. Newton of the University of California San Diego, La Jolla, CA for the generous gift of the PHLPP-specific inhibitor, NCS 45586 (#13).

REFERENCES

- Weisiger, R. A., and Fridovich, I. (1973) *J. Biol. Chem.* **248**, 4793–4796
- Fridovich, I. (1995) *Annu. Rev. Biochem.* **64**, 97–112
- Fridovich, I. (1978) *Science* **201**, 875–880
- Li, Y., Huang, T. T., Carlson, E. J., Melov, S., Ursell, P. C., Olson, J. L., Noble, L. J., Yoshimura, M. P., Berger, C., Chan, P. H., Wallace, D. C., and Epstein, C. J. (1995) *Nat. Genet.* **11**, 376–381
- Oberley, L. W., and Buettner, G. R. (1979) *Cancer Res.* **39**, 1141–1149
- St Clair, D. K., Wan, X. S., Oberley, T. D., Muse, K. E., and St Clair, W. H. (1992) *Mol. Carcinog.* **6**, 238–242
- Church, S. L., Grant, J. W., Ridnour, L. A., Oberley, L. W., Swanson, P. E., Meltzer, P. S., and Trent, J. M. (1993) *Proc. Natl. Acad. Sci. U.S.A.* **90**, 3113–3117
- Wong, G. H., and Goeddel, D. V. (1988) *Science* **242**, 941–944
- Wong, G. H., Elwell, J. H., Oberley, L. W., and Goeddel, D. V. (1989) *Cell* **58**, 923–931
- Visner, G. A., Dougall, W. C., Wilson, J. M., Burr, I. A., and Nick, H. S. (1990) *J. Biol. Chem.* **265**, 2856–2864
- Harris, C. A., Derbin, K. S., Hunte-McDonough, B., Krauss, M. R., Chen, K. T., Smith, D. M., and Epstein, L. B. (1991) *J. Immunol.* **147**, 149–154
- Fujii, J., and Taniguchi, N. (1991) *J. Biol. Chem.* **266**, 23142–23146
- Whitsett, J. A., Clark, J. C., Wispe, J. R., and Pryhuber, G. S. (1992) *Am. J. Physiol.* **262**, L688–693
- Oberley, L. W., St Clair, D. K., Autor, A. P., and Oberley, T. D. (1987) *Arch. Biochem. Biophys.* **254**, 69–80
- Akashi, M., Hachiya, M., Paquette, R. L., Osawa, Y., Shimizu, S., and Suzuki, G. (1995) *J. Biol. Chem.* **270**, 15864–15869
- Yeh, C. C., Wan, X. S., and St Clair, D. K. (1998) *DNA Cell Biol.* **17**, 921–930
- Xu, Y., Porntadavity, S., and St Clair, D. K. (2002) *Biochem. J.* **362**, 401–412
- Dhar, S. K., Xu, Y., Chen, Y., and St Clair, D. K. (2006) *J. Biol. Chem.* **281**, 21698–21709
- Porntadavity, S., Xu, Y., Kiningham, K., Rangnekar, V. M., Prachayasittikul, V., and St Clair, D. K. (2001) *DNA Cell Biol.* **20**, 473–481
- Xu, Y., Krishnan, A., Wan, X. S., Majima, H., Yeh, C. C., Ludewig, G., Kasarskis, E. J., and St Clair, D. K. (1999) *Oncogene* **18**, 93–102
- Zhu, C. H., Huang, Y., Oberley, L. W., and Domann, F. E. (2001) *J. Biol. Chem.* **276**, 14407–14413
- Xu, Y., Fang, F., Dhar, S. K., Bosch, A., St Clair, W. H., Kasarskis, E. J., and St Clair, D. K. (2008) *Mol. Cancer Res.* **6**, 1881–1893
- Jones, P. L., Ping, D., and Boss, J. M. (1997) *Mol. Cell Biol.* **17**, 6970–6981
- Xu, Y., Kiningham, K. K., Devalaraja, M. N., Yeh, C. C., Majima, H., Kasarskis, E. J., and St Clair, D. K. (1999) *DNA Cell Biol.* **18**, 709–722
- Kiningham, K. K., Xu, Y., Daosukho, C., Popova, B., and St Clair, D. K. (2001) *Biochem. J.* **353**, 147–156
- Dhar, S. K., Lynn, B. C., Daosukho, C., and St Clair, D. K. (2004) *J. Biol. Chem.* **279**, 28209–28219
- Kim, H. P., Roe, J. H., Chock, P. B., and Yim, M. B. (1999) *J. Biol. Chem.* **274**, 37455–37460
- Nishizuka, Y. (1984) *Nature* **308**, 693–698
- Cerutti, P. A. (1985) *Science* **227**, 375–381
- Das, K. C., Guo, X. L., and White, C. W. (1998) *J. Biol. Chem.* **273**, 34639–34645
- Kiningham, K. K., Daosukho, C., and St Clair, D. K. (2004) *Biochem. J.* **384**, 543–549
- Storz, P., Döppler, H., and Toker, A. (2005) *Mol. Cell Biol.* **25**, 8520–8530
- Kops, G. J., Dansen, T. B., Polderman, P. E., Saarloos, I., Wirtz, K. W., Coffey, P. J., Huang, T. T., Bos, J. L., Medema, R. H., and Burgering, B. M. (2002) *Nature* **419**, 316–321
- Calnan, D. R., and Brunet, A. (2008) *Oncogene* **27**, 2276–2288
- Sierecki, E., Sinko, W., McCammon, J. A., and Newton, A. C. (2010) *J. Med. Chem.* **53**, 6899–6911
- Enoksson, M., Robertson, J. D., Gogvadze, V., Bu, P., Kropotov, A., Zhivotovsky, B., and Orrenius, S. (2004) *J. Biol. Chem.* **279**, 49575–49578
- Chung, Y. W., Jeong, D. W., Won, J. Y., Choi, E. J., Choi, Y. H., and Kim, I. Y. (2002) *Biochem. Biophys. Res. Commun.* **293**, 1248–1253
- Jeong, D. W., Yoo, M. H., Kim, T. S., Kim, J. H., and Kim, I. Y. (2002) *J. Biol. Chem.* **277**, 17871–17876
- Chun, J. Y., Kim, K. J., Hwang, I. T., Kim, Y. J., Lee, D. H., Lee, I. K., and Kim, J. K. (2007) *Nucleic Acids Res.* **35**, e40
- Riganti, C., Gazzano, E., Polimeni, M., Costamagna, C., Bosia, A., and Ghigo, D. (2004) *J. Biol. Chem.* **279**, 47726–47731
- Brunet, A., Bonni, A., Zigmond, M. J., Lin, M. Z., Juo, P., Hu, L. S., Anderson, M. J., Arden, K. C., Blenis, J., and Greenberg, M. E. (1999) *Cell* **96**, 857–868
- Wen, H. C., Huang, W. C., Ali, A., Woodgett, J. R., and Lin, W. W. (2003) *Cell Signal* **15**, 37–45
- Li, L., Sampat, K., Hu, N., Zakari, J., and Yuspa, S. H. (2006) *J. Biol. Chem.* **281**, 3237–3243
- Millward, T. A., Zolnierowicz, S., and Hemmings, B. A. (1999) *Trends Biochem. Sci.* **24**, 186–191
- Rocher, G., Letourneux, C., Lenormand, P., and Porteu, F. (2007) *J. Biol. Chem.* **282**, 5468–5477
- Ishihara, H., Martin, B. L., Brautigam, D. L., Karaki, H., Ozaki, H., Kato, Y., Fusetani, N., Watabe, S., Hashimoto, K., Uemura, D., et al. (1989) *Biochem. Biophys. Res. Commun.* **159**, 871–877
- Singh, A., Ye, M., Bucur, O., Zhu, S., Tanya Santos, M., Rabinovitz, I., Wei, W., Gao, D., Hahn, W. C., and Khosravi-Far, R. (2010) *Mol. Biol. Cell* **21**, 1140–1152
- Gao, T., Furnari, F., and Newton, A. C. (2005) *Mol. Cell* **18**, 13–24
- Drane, P., Bravard, A., Bouvard, V., and May, E. (2001) *Oncogene* **20**, 430–439
- Brindle, P., Linke, S., and Montminy, M. (1993) *Nature* **364**, 821–824
- Mayr, B., and Montminy, M. (2001) *Nat. Rev. Mol. Cell Biol.* **2**, 599–609
- Muthusamy, N., and Leiden, J. M. (1998) *J. Biol. Chem.* **273**, 22841–22847
- Ramaswamy, S., Nakamura, N., Sansal, I., Bergeron, L., and Sellers, W. R. (2002) *Cancer Cell* **2**, 81–91
- Medema, R. H., Kops, G. J., Bos, J. L., and Burgering, B. M. (2000) *Nature* **404**, 782–787
- Kuo, Y. C., Huang, K. Y., Yang, C. H., Yang, Y. S., Lee, W. Y., and Chiang, C. W. (2008) *J. Biol. Chem.* **283**, 1882–1892